Analytical Methods

ROYAL SOCIETY OF CHEMISTRY

PAPER

View Article Online
View Journal | View Issue

Cite this: *Anal. Methods*, 2025, **17**, 8460

Optimization of headspace extraction conditions for volatile hydrocarbons from aqueous matrices using experimental design approaches

Fabrizio Ruggieri, *[a] Milena Casalena,[a] Mariagiovanna Accili,[a] Elisa Mattei,[b] Fabrizio Stecca[b] and Mosè Lamolinara[b]

This study presents a robust, statistically validated analytical method for the quantification of C5–C10 volatile petroleum hydrocarbons (VPHs) in aqueous matrices using headspace gas chromatography with flame ionization detection (HS-GC-FID). A central composite face-centered (CCF) experimental design was employed to optimize critical extraction parameters, including sample volume, temperature, and equilibration time. The response variable, defined as the chromatographic peak area per microgram of analyte (Area per μg), was used to model the extraction efficiency. Analysis of variance (ANOVA) confirmed the global significance of the fitted model (R^2 = 88.86%, RMSE = 4.997, p < 0.0001), with significant main, quadratic, and interaction effects. Sample volume showed the strongest negative impact, while temperature and interaction terms demonstrated synergistic behavior. The optimized conditions improved both sensitivity and reproducibility. The proposed method aligns with ISO 9377-2 principles and provides a reliable, environmentally relevant protocol for trace-level VPH monitoring in water samples.

Received 14th July 2025
Accepted 1st October 2025

DOI: 10.1039/d5ay01147g

rsc.li/methods

1 Introduction

Volatile petroleum hydrocarbons (VPHs) encompass a range of low molecular weight aliphatic compounds, including linear and branched alkanes typically found in gasoline and other petroleum-derived fuels. These substances, spanning from 2-methylpentane to *n*-decane, are classified as environmentally hazardous due to their persistence, volatility, and potential toxicity. Their release into the environment through industrial activities, spills, and fuel leakage results in widespread contamination of groundwater and surface waters.[1–3] Exposure to these compounds has been linked to both acute and chronic toxicological effects, prompting the implementation of stringent environmental monitoring requirements.[4–6]

Accurate and sensitive determination of VPHs in aqueous samples is a critical component of environmental surveillance and public health protection. In this context, the ISO 9377-2:2000 standard outlines a reference method for the determination of hydrocarbons in water using gas chromatography, with particular emphasis on the quantification of extractable and volatile fractions.[7,8] This international guideline provides criteria for method validation, quality control, and analytical performance, emphasizing the need for reproducibility, recovery efficiency, and the ability to detect hydrocarbons in complex aqueous matrices.[9–12] The method described in the present study aligns with the technical principles and objectives of ISO 9377-2, aiming to offer a statistically validated, reproducible alternative tailored to volatile hydrocarbons (C5–C10) that are typically not covered by standard extraction protocols.[13] Regulatory bodies such as the U.S. Environmental Protection Agency (EPA) and the European Union have developed standardized protocols, including EPA Method 8015 and the European Water Framework Directive (2000/60/EC), to guide analytical practices.[14,15] These frameworks mandate the use of reliable, reproducible, and sensitive methods capable of detecting VPHs at trace levels in complex aqueous matrices.[16,17]

Among the various analytical strategies available, headspace gas chromatography coupled with flame ionization detection (HS-GC-FID) remains one of the most effective and widely used techniques for the quantification of volatile hydrocarbons.[18–20] HS-GC-FID offers distinct advantages in terms of sample cleanliness, ease of automation, and compatibility with volatile organic compounds. However, the accuracy and sensitivity of HS-GC-FID measurements are highly dependent on the optimization of experimental parameters such as sample volume, headspace equilibration temperature, and extraction time.[21–24] These variables influence the distribution of analytes between the aqueous and vapor phases and can significantly affect signal response and reproducibility.[25–27]

To address this challenge, the current study employs a multivariate statistical approach based on design of

[a]*Dipartimento di Scienze Fisiche e Chimiche, Università degli Studi dell'Aquila, Via Vetoio, 67010 Coppito, L'Aquila, Italy. E-mail: fabrizio.ruggieri@univaq.it*
[b]*Agenzia Regionale per la Protezione dell' Ambiente (ARPA) Abruzzo, 67100 L'Aquila, Italy*

experiments (DoE) to optimize HS-GC-FID extraction conditions for VPHs in water.[28] Unlike the traditional one-variable-at-a-time (OVAT) methodology, which fails to account for synergistic effects and often leads to inefficient and incomplete optimization, DoE allows for the simultaneous assessment of multiple factors and their interactions. This enables the construction of predictive mathematical models and facilitates a more thorough understanding of the extraction dynamics. A central composite face-centered (CCF) design was selected for its efficiency and capability to model curvature and interaction effects.

The use of DoE not only enhances experimental efficiency by reducing the number of required runs but also strengthens statistical confidence in identifying significant variables.[29] This approach is especially valuable in complex analytical systems, where multiple interdependent parameters govern method performance.[30–33] Through this framework, the present study aims to derive scientifically validated optimal conditions and to highlight the utility of DoE as a powerful tool in analytical method development.[34,35]

The objective of this research is to develop a robust, reproducible, and environmentally relevant analytical protocol for the quantification of volatile petroleum hydrocarbons (VPHs, C5–C10) in water samples. Current international standards do not adequately cover this fraction: the ISO 9377-2 method is based on liquid–liquid extraction (LLE) and was designed mainly for heavier hydrocarbons, U.S. EPA Method 8015 relies on purge-and-trap strategies, and the European Water Framework Directive (2000/60/EC) establishes monitoring requirements without prescribing headspace protocols. In this context, our study addresses a methodological gap by developing and statistically optimizing a headspace-based HS-GC-FID procedure specifically for volatile hydrocarbons. The application of a CCF design allowed us to elucidate the influence of key extraction parameters, improve sensitivity and precision, and capture interaction effects not revealed by traditional OVAT approaches. The advantages of the proposed protocol include full automation, reduced solvent consumption, enhanced reproducibility, and compliance with international performance criteria, ultimately contributing to the development of reliable tools for regulatory monitoring and environmental risk assessment.Beyond controlled experiments on spiked ultrapure water, the optimized HS-GC-FID protocol was also applied to real groundwater samples, confirming its practical applicability for environmental monitoring and its alignment with international regulatory frameworks.

2 Experimental

2.1 Reagents and standards

Analytical-grade standards of C5–C10 hydrocarbons were dissolved in methanol to prepare stock and working solutions. These included linear and branched alkanes representative of petroleum volatile hydrocarbon fractions. Calibration solutions were prepared in methanol to cover a concentration range of 0.1 to 20 μg mL^{-1}, ensuring linear response over two orders of magnitude. Serial dilutions were carried out using methanol in class. A volumetric glassware to maintain volumetric accuracy. Ultrapure water (18.2 MΩ cm), produced using a Milli-Q system (Millipore), was employed for all sample preparations, dilutions, and blank determinations to eliminate potential background contamination. All reagents and solvents were verified to be free of target analytes by blank analysis.

2.2 Instrumentation

Gas chromatographic analyses were carried out using an Agilent 6890 system equipped with a flame ionization detector (FID) and a DB-1 fused-silica capillary column (30 m × 0.25 mm i.d. × 1.0 μm film thickness), selected for its non-polar stationary phase suitable for hydrocarbon separation. The system was coupled to a static headspace sampler (Agilent G1888), which enabled automated vial incubation, headspace pressurization, and sample injection. The autosampler was fully programmable for equilibration temperature, equilibration time, pressurization time, and injection volume, ensuring precise and reproducible sample handling. Headspace injections were performed in split mode (5 : 1 split ratio), with a fixed injection volume of 1.0 mL of vapor phase introduced into the GC inlet The GC oven program was 40 °C hold for 2 min and successively ramped linearly to 180 °C over 12 min with a final hold of 1 min, for a total run time of 13 min; injector temperature 250 °C; detector temperature 300 °C; carrier gas helium at 1.2 mL min^{-1}. The GC oven, injector, and detector parameters were optimized to achieve sharp peak resolution and linear detector response across the tested concentration range. Routine maintenance and performance checks, including septum integrity, leak testing, and detector calibration, were conducted to ensure data quality and instrumental reliability throughout the experimental campaign.

2.3 Sample preparation

For each experimental run, water samples were freshly prepared by transferring a defined volume of ultrapure water (18.2 MΩ cm) into 20 mL headspace vials, followed by spiking with hydrocarbon standards to reach the desired analyte concentration. The spiking procedure was designed to minimize the amount of organic solvent introduced into the aqueous samples. The final concentration of methanol in the headspace vials never exceeded 1% v/v and was kept constant across all experimental runs. This level is sufficiently low to avoid significant alterations of analyte partitioning behavior in the aqueous-headspace equilibrium, while ensuring comparability of results and excluding solvent-related biases. Each water sample was fortified with the appropriate volume of the reference material supplemented with 1.8 g of sodium chloride (NaCl) and 10 μL of methanol. Procedural blanks were prepared using the same reagents and glassware employed for matrix spikes, in order to guarantee strictly comparable conditions. The consistent addition of NaCl improved analyte partitioning efficiency into the headspace and enhanced method reproducibility.

The vials were immediately sealed with PTFE/silicone septa and aluminum crimp caps to prevent analyte loss. Stirring during equilibration was not included, as the Agilent 7697A autosampler does not allow vial agitation. Sample volume (V),

incubation temperature (T), and equilibration time (t) were varied systematically according to the experimental design matrix. All samples were equilibrated in the headspace autosampler oven prior to injection into the GC system. Replicates were included at the center point of the design to assess repeatability and estimate pure error. Blanks and quality control samples were analyzed in parallel to monitor for contamination and assess method performance.

2.4 Analytical procedure validation

The analytical procedure was validated following ISO 9377-2:2000 and International Conference on Harmonization ICH Q2(R1) guidelines, with an expanded focus on linearity, sensitivity, precision, accuracy, robustness, and model adequacy. Validation was conducted on standard mixtures of C5–C10 hydrocarbons using the optimized HS-GC-FID protocol to confirm the method's scientific reliability and regulatory fitness for environmental applications.

The linearity was assessed over a concentration range of 0.1–20 μg mL^{-1} using six replicate injections per level.

The precision of the method was evaluated through comprehensive intra-day and inter-day studies to assess method repeatability and reproducibility. Intra-day precision was assessed by performing six replicate injections at three concentration levels (0.5, 5, and 15 μg mL^{-1}) within a single day, while inter-day precision was assessed by repeating the same procedure across three consecutive days.

The accuracy of method was determined through recovery experiments by spiking blank water samples with standard mixtures of C5–C10 hydrocarbons at three concentration levels: low (0.5 μg mL^{-1}), medium (5 μg mL^{-1}), and high (15 μg mL^{-1}). Each level was analyzed in six replicates to ensure statistical reliability. The method sensitivity was rigorously assessed following ICH Q2(R1) guidelines by determining the limit of detection (LOD) and limit of quantification (LOQ) using the calibration curve approach. The standard deviation of the response ($\sigma = 0.153$), derived from multiple blank injections, and the slope of the calibration curve ($S = 124.78$) were used in the formulas $LOD = 3.3\sigma/S$ and $LOQ = 10\sigma/S$. The robustness was evaluated by deliberately varying method parameters (±2 °C equilibration temperature and ±2 min extraction time).

2.5 Experimental design

A central composite face-centered (CCF) design was employed to optimize the extraction conditions in headspace gas chromatography for volatile hydrocarbons. This design allows for efficient exploration of the experimental space and provides the ability to model both linear and quadratic effects as well as interactions between variables. The three selected independent variables, extraction temperature (X_1), equilibration time (X_2), and sample volume (X_3), were each tested at three levels (low, center, and high).

Replicates were performed with variable frequency (two or three runs) to allow estimation of both intra-day and inter-day error, thereby improving the robustness of the statistical model. The inclusion of replicates allowed for the estimation of pure experimental error and improved the robustness of the model by enabling the detection of lack-of-fit. The response variable was defined as the total chromatographic peak area per microgram of analyte (Area per μg), obtained from GC-FID analysis. The response variable was defined as the sum of normalized chromatographic peak areas per microgram of analyte for the C5–C10 hydrocarbons, thus providing a global measure of extraction efficiency. Regarding calibration, petroleum hydrocarbon methods commonly adopt a range-based approach for gasoline range organics or total petroleum hydrocarbons, calibrating with a representative petroleum standard and integrating the total area over the specified carbon window rather than requiring compound-specific calibration for every constituent. This practice is documented for EPA and ISO 9377-2. This statistical structure is particularly suited for response surface methodology (RSM) and facilitates the construction of a second-order polynomial model that captures both curvature and interaction effects.

This normalized measure served as a quantitative indicator of the extraction efficiency under varying experimental conditions, accounting for differences in analyte concentration and ensuring consistency across the design space. The data were subjected to analysis of variance (ANOVA) to evaluate the statistical significance of main effects, interaction terms, and quadratic contributions. Model accuracy and predictive reliability were assessed using the root mean square error (RMSE) and the coefficient of determination (R^2). This rigorous design and analysis strategy ensured a comprehensive understanding of the influence of experimental variables on the analytical response and facilitated the identification of robust and optimized extraction conditions.

3 Results and discussion

3.1 Model validation

The experimental dataset generated through the central composite face-centered (CCF) design is presented in Table 1, where the investigated variables, their tested levels, and the corresponding response values are reported. The design included 27 randomized experimental runs covering the full factorial and axial points, complemented by 19 replicated center points to provide an estimate of pure error and to assess method repeatability. The randomization of the experimental order minimized potential bias arising from uncontrolled external factors, while the replicated measurements at the center of the design space ensured that the statistical analysis was based on reproducible data. This comprehensive dataset formed the basis for the development of a second-order polynomial model capable of describing both main effects and interaction terms, ultimately supporting the identification of optimal extraction conditions.

Analysis of variance (ANOVA) confirmed the model's global significance, with a high coefficient of determination ($R^2 = 89.1\%$) and adjusted R^2 of 86.9%, indicating a reliable model fit to the data, as shown in Table 2. The root mean square error (RMSE) of 4972 supports the low dispersion of residuals. The inclusion of numerous replicates allowed accurate estimation

Table 1 CCF investigated experimental factors in coded and actual form, and experimental responses. Asterisks (*) indicate replicated runs used to assess experimental reproducibility

	Independent variable (coded form)			Indipendent variable (actual form)			
Run	X_1	X_2	X_3	T (°C)	t (min)	V (mL)	Response (peak area per μg)
1	−1	−1	−1	60	15	4	94.012
2*	−1	−1	−1	60	15	4	98.321
3	−1	−1	0	60	15	7	61.133
4	−1	−1	1	60	15	10	51.817
5*	−1	−1	1	60	15	10	56.651
6*	−1	−1	1	60	15	10	55.011
7	−1	0	−1	60	20	4	92.226
8	−1	0	0	60	20	7	64.579
9*	−1	0	0	60	20	7	68.815
10*	−1	0	0	60	20	7	71.797
11	−1	0	1	60	20	10	57.626
12	−1	1	−1	60	25	4	78.835
13*	−1	1	−1	60	25	4	79.904
14	−1	1	0	60	25	7	50.145
15	−1	1	1	60	25	10	60.552
16*	−1	1	1	60	25	10	65.519
17*	−1	1	1	60	25	10	62.943
18	0	−1	−1	70	15	4	99.689
19	0	−1	0	70	15	7	62.488
20	0	−1	1	70	15	10	60.551
21	0	0	−1	70	20	4	86.064
22*	0	0	−1	70	20	4	80.705
23*	0	0	−1	70	20	4	89.424
24	0	0	0	70	20	7	71.035
25	0	0	1	70	20	10	66.085
26*	0	0	1	70	20	10	68.121
27*	0	0	1	70	20	10	70.885
28	0	1	−1	70	25	4	77.183
29	0	1	0	70	25	7	46.319
30	0	1	1	70	25	10	69.976
31	1	−1	−1	80	15	4	100.96
32*	1	−1	−1	80	15	4	94.284
33	1	−1	0	80	15	7	68.951
34	1	−1	1	80	15	10	67.532
35	1	0	−1	80	20	4	91.096
36	1	0	0	80	20	7	73.705
37*	1	0	0	80	20	7	78.982
38*	1	0	0	80	20	7	75.629
39	1	0	1	80	20	10	67.722
40	1	1	−1	80	25	4	61.354
41*	1	1	−1	80	25	4	77.088
42*	1	1	−1	80	25	4	65.868
43	1	1	0	80	25	7	51.461
44	1	1	1	80	25	10	67.690
45*	1	1	1	80	25	10	68.459
46*	1	1	1	80	25	10	71.460

of pure error and improved the model's diagnostic capability, particularly in detecting curvature and interactions.

The regression coefficients revealed statistically significant effects for the main factors (temperature, extraction time, and sample volume), with the volume of the aqueous phase (X_3) showing the strongest negative effect (−9.3, $p < 0.0001$).

Table 2 Regression coefficients and ANOVA summary from the central composite face-centered design applied to headspace extraction. Statistically significant terms ($p < 0.05$) are reported, along with model performance metrics (R^2, adjusted R^2, Q^2) and ANOVA statistics

Parameters	Value ± SD	R^2	Adj-R^2	Q^2
Intercept	67.9 ± 1.6			
X_2	2.0 ± 0.8			
X_2	−5.5 ± 0.9			
X_3	−9.3 ± 0.9			
$X_1 \cdot X_2$	−2.3 ± 1.1	0.891	0.868	0.811
$X_1 \cdot X_3$	3.4 ± 1.9			
$X_2 \cdot X_3$	7.3 ± 1.1			
X_2^2	−6.3 ± 1.6			
X_3^2	12.0 ± 1.7			

Variation source	Sum of squares	Degrees of freedom	Mean square	F-value	p-value
Lack of fit	612.81	18	34.04	2.1423	00 541
Pure error	301.94	19	15.89		
Model	7496.47	8	937.06	37.90	<00 001
Residual	914.76	37	24.72		

Interaction terms ($T \cdot V$, $t \cdot V$) and quadratic effects (t^2, V^2) were also significant, confirming non-linearity and factor interplay in the extraction process. Calculated *vs.* actual plots demonstrated excellent correlation with no apparent systematic deviations as reported in Fig. 1.

The scatter plot demonstrates a strong linear relationship between the actual and calculated values of the extraction response (Area per μg), with minimal dispersion around the regression line. This high degree of alignment confirms the model's predictive capability and indicates that the majority of the experimental variability is well captured by the model.

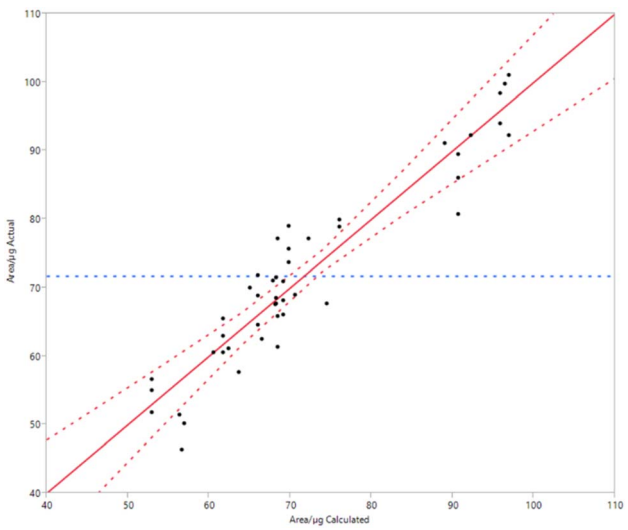

Fig. 1 Correlation plot between actual and calculated extraction responses (Area per μg) based on the fitted response surface model. The solid red line represents the linear regression fit, while the dashed red lines denote the confidence intervals.

3.2 Variable effects

The three-dimensional response surfaces reveal how temperature and sample volume jointly influence extraction efficiency under different equilibration times. Across all time levels, sample volume (X_3) exerts a consistently negative effect on response, indicating that lower sample volumes enhance analyte transfer to the gas phase. This is primarily attributed to the increased headspace-to-liquid ratio, which favors the volatilization of hydrophobic compounds in accordance with Henry's law. In headspace analysis, the distribution of volatile compounds between the aqueous and gas phases is governed by the equilibrium constant defined by Henry's law coefficient.

Lowering the sample volume shifts this equilibrium toward the gas phase, thereby increasing the analyte concentration in the headspace and consequently the GC-FID signal. Moreover, reduced liquid volumes may also decrease matrix effects and lower the solvation energy barrier for analyte release, further enhancing extraction efficiency. These effects become especially relevant in the analysis of moderately volatile hydrocarbons, where partitioning dynamics are sensitive to even small variations in liquid-phase volume. Therefore, the systematic negative correlation between volume and response is both thermodynamically and kinetically justified.

From a practical perspective, the graphical shape of the response surfaces also provides visual confirmation of experimental robustness. The presence of wide and smooth maximum regions, especially at 20 minutes, suggests that the optimized conditions are not acutely sensitive to small deviations in volume or temperature. This characteristic is desirable in routine environmental analyses, where minor procedural fluctuations may occur. Moreover, the curvature and tilt of the surfaces offer mechanistic insight: sharp peaks or valleys would imply strong local sensitivity and potential instability, whereas gently sloping optima indicate more forgiving conditions. Thus, these surface plots are not only predictive but also diagnostically valuable, enabling the analyst to balance efficiency with operational resilience.

At short extraction time (Fig. 2), the response is predominantly governed by the sample volume effect, with temperature contributing marginally to the signal intensity. This behavior suggests that the system has not yet reached full thermodynamic equilibrium between the aqueous and headspace phases. Under these conditions, the volatilization of analytes is driven primarily by the headspace-to-liquid ratio, as governed by Henry's law, but the lower exposure time restricts the ability of thermal agitation to enhance mass transfer. As a result, temperature-induced increases in vapor pressure are not fully realized, and the thermal equilibrium necessary for optimal analyte desorption is likely incomplete.

Consequently, kinetic limitations dominate the extraction dynamics at short equilibration times, minimizing the observable influence of temperature.

In Fig. 3 response surface is reported with X_2 fixed at an intermediate level; a synergistic interaction between temperature and volume becomes evident.

The response surface displays a well-defined optimal region, where moderate temperatures and low sample volumes ($X_3 < 0$) lead to the highest extraction efficiency. This configuration enhances both the volatilization kinetics and the equilibrium partitioning of the analytes. At 20 minutes, the system likely approaches thermodynamic equilibrium, allowing the elevated temperature to significantly increase analyte vapor pressures and thus their transfer into the headspace. Simultaneously, the reduced liquid volume maintains a favorable headspace-to-liquid ratio, maximizing mass transfer. These concurrent effects confirm the joint role of temperature-induced vapor

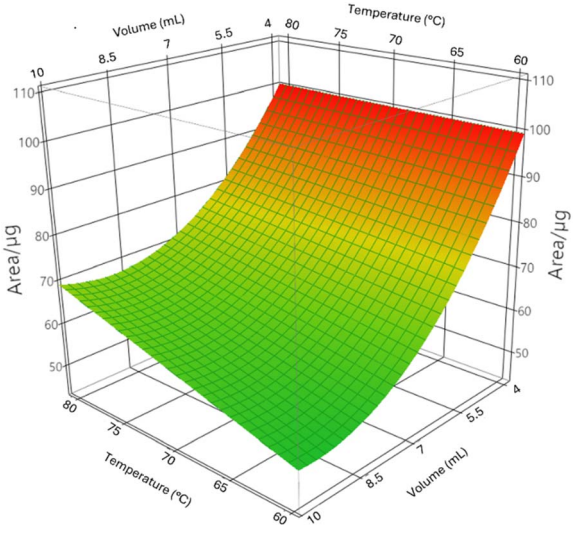

Fig. 2 Response surface plot showing the effect of sample volume and extraction temperature on HS-GC-FID response (Area per µg), with equilibration time fixed at 15 min. The plot indicates that lower sample volumes combined with higher extraction temperatures enhance headspace partitioning efficiency and yield higher analytical responses.

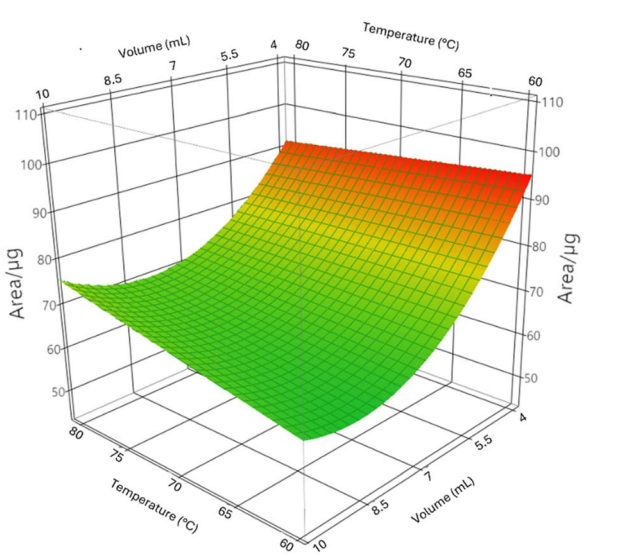

Fig. 3 Response surface plot showing the effect of sample volume and extraction temperature on HS-GC-FID response (Area per µg), with equilibration time fixed at 20 min.

pressure increase and volume-controlled phase distribution, yielding a cooperative enhancement of the extraction yield.

At $t = 25$ min, as reported in Fig. 4, the overall GC-FID response decreases slightly and the response surface becomes notably flatter, especially at higher temperatures. This trend reflects a non-linear effect of extraction time, where prolonged equilibration does not further enhance analyte partitioning and may in fact lead to marginal losses in signal intensity. Such losses could arise from volatilization beyond the optimal headspace saturation point, condensation of higher boiling compounds on cooler vial walls, or sample leek. Under these conditions, the system is likely to have surpassed its thermodynamic optimum, where analyte partitioning into the vapor phase is no longer favored.

Prolonged equilibration may also introduce kinetic disturbances, potentially shifting or destabilizing the equilibrium previously attained, thereby compromising extraction efficiency and analytical reproducibility.

The observed flattening suggests that prolonged heating no longer contributes positively to analyte recovery and may introduce variance. The positive curvature associated with the X_3^2 term supports this observation, revealing that very low sample volumes under these conditions may lead to reduced reproducibility, possibly due to increased susceptibility to vapor-phase variability or edge effects within the vial.

Taken together, these surfaces underscore the critical role of not only optimizing individual experimental variables but also understanding their synergistic and antagonistic interactions. The presence of significant interaction and quadratic terms in the fitted model highlights the complexity of the headspace extraction system, where temperature, time, and volume exert interdependent effects on analyte volatilization and partitioning dynamics. Among the conditions evaluated, the intermediate extraction time of 20 minutes provides the most favorable balance between efficient mass transfer and signal stability. This setting allows sufficient time for the system to approach equilibrium while minimizing potential losses due to overexposure or degradation, thus maximizing both analytical sensitivity and method robustness.

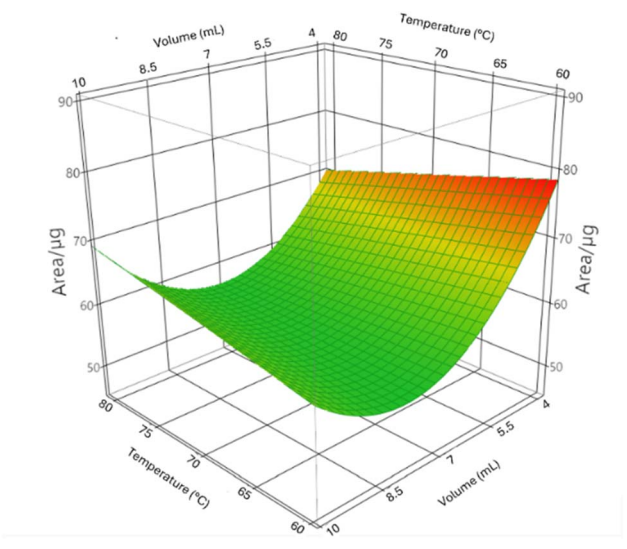

Fig. 4 Three-dimensional response surface plot illustrating the combined effect of sample volume and extraction temperature on the analytical response (Area per µg) obtained by HS-GC-FID, with the equilibration time fixed at 25 min.

3.3 Analytical procedure validation

Method validation was performed under the optimized conditions identified by the DoE (70 °C, 15 min equilibration time and 4 mL sample volume). The resulting calibration curve exhibited excellent linearity, with a regression slope (b) of 124.78 and intercept (a) of 35.06. The coefficient of determination ($R^2 = 0.998$) confirms a strong linear correlation. Model fit was further supported by a low residual sum of squares (RSS = 6.10) relative to the total sum of squares (TSS = 3256.45). Residuals were normally distributed (Shapiro–Wilk $p > 0.05$), supporting the suitability of the linear model across the tested range. Relative standard deviations (RSDs), calculated to evaluate the precision, were consistently below 4.5% for intra-day and below 6.5% for inter-day experiments, meeting the acceptability criteria recommended by ISO and ICH guidelines. These findings demonstrate the method's capability to deliver consistent and reproducible results across multiple days and concentration levels, highlighting its robustness for routine environmental monitoring. Mean recoveries ranged from 94.2% to 101.8%, with standard deviations below 4.5%, confirming consistent recovery of analytes across the calibration range. To evaluate matrix effects, spiked river water samples and procedural blanks were analyzed in parallel. Mean recoveries ranged from 92% to 105%, with RSD values below 7%, confirming that matrix effects were negligible under the optimized conditions. These results indicate that the method accurately reflects the true analyte concentration and complies with accepted performance criteria for environmental methods. Furthermore, no matrix effects were observed, and blank samples confirmed the absence of background interferences. This confirms the method's robustness and reliability for quantifying trace-level hydrocarbons in aqueous samples. The calculated limits of detection (LOD) and quantification (LOQ) were 0.040 µg mL^{-1} and 0.123 µg mL^{-1}, respectively, demonstrating the high sensitivity of the optimized HS-GC-FID protocol and its suitability for trace-level analysis of volatile hydrocarbons in aqueous matrices. In addition, recoveries ranged from 92% to 105% with relative standard deviations (RSDs) consistently below 6.5%, confirming the robustness and reproducibility of the method. Collectively, these results not only fall well within the requirements established by ISO 9377-2 for hydrocarbon monitoring in water (recoveries 70–120%, RSD < 10%, LOQ ≤ 0.2 µg mL^{-1}), but also demonstrate that the proposed protocol provides performance fully compliant with, and in some aspects superior to, international regulatory standards. In addition, robustness tests showed negligible influence on the analytical signal (RSD < 5%), supporting the stability of the method against small operational fluctuations. The obtained detection limit (0.04 µg mL^{-1}) is comparable to those typically achieved in accredited environmental laboratories for routine monitoring

of hydrocarbons in water, confirming the adequacy of the method for trace analysis. Although purge-and-trap techniques may provide slightly lower limits, they involve more complex instrumentation and higher operational costs. The proposed HS-GC-FID protocol, therefore, represents a reliable and sustainable alternative, fully compliant with ISO performance criteria and suitable for environmental applications. Having established the sensitivity, precision, and robustness of the optimized protocol, the method was further evaluated on real water matrices to confirm its practical applicability under environmental monitoring conditions.

3.4 Analysis of real groundwater samples

The applicability of the optimized HS-GC-FID protocol was further evaluated by analyzing three groundwater samples. A representative chromatogram is reported in Fig. 5, where the target hydrocarbons are clearly resolved within the defined integration windows. In the first sample, the measured concentrations were 1.95 mg L^{-1} for *n*-pentane, 0.10 mg L^{-1} for *n*-hexane, 0.10 mg L^{-1} for *n*-heptane, 0.12 mg L^{-1} for *n*-nonane, and 0.06 mg L^{-1} for *n*-undecane, while the remaining compounds of interest were below the respective LODs.

The other two samples displayed analogous patterns, with detectable hydrocarbons limited to a few analytes and at concentrations generally close to the low μg L^{-1} range.

These results confirm that the method is fully applicable to real environmental matrices and capable of detecting and quantifying volatile hydrocarbons even in complex aqueous samples without additional pre-treatment. The concentrations observed, particularly for *n*-pentane, reflect the high volatility and environmental mobility of the lighter hydrocarbons, which are among the most frequently encountered contaminants in groundwater impacted by fuel leaks and industrial emissions. Importantly, the method achieved quantification well within the limits established by international standards, with accuracy and reproducibility consistent with ISO 9377-2 requirements.

Overall, the successful application to real groundwater samples demonstrates that the optimized HS-GC-FID protocol is not only statistically robust under controlled experimental conditions but also reliable and effective in routine environmental monitoring scenarios.

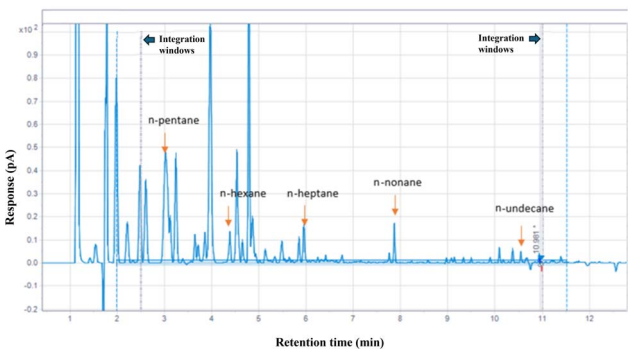

Fig. 5 HS-GC-FID chromatogram of a representative groundwater sample showing quantified hydrocarbons; other analytes were below the LOD.

4 Conclusions

This study presents a scientifically robust and statistically validated HS-GC-FID protocol for the quantification of C5–C10 volatile hydrocarbons in aqueous matrices, tailored to the demanding requirements of environmental monitoring. The application of a central composite face-centered experimental design enabled an exhaustive investigation of the effect of sample volume, extraction temperature, and equilibration time on analytical performance. Among these, sample volume emerged as the most influential factor, significantly impacting the headspace partitioning efficiency of volatile analytes. The positive and significant effects of extraction temperature and interaction terms such as $t \cdot V$ and $T\ V$ further confirmed the relevance of synergistic and nonlinear behavior in the extraction process.

The method's optimization resulted in improved extraction efficiency, reproducibility, and predictive reliability, as supported by strong statistical parameters ($R^2 = 88.86\%$, RMSE = 4.997, $p < 0.0001$). The validated response surface model accurately predicts analytical behavior within the tested domain and permits valuable guidance for method transferability and routine application. These findings underscore the importance of integrating experimental design strategies into analytical method development, enabling precise control of key variables and improving the robustness of determinations in environmental matrices.

This work advances the development of environmentally relevant analytical methods by introducing a model-driven and statistically validated framework for optimizing sample preparation in headspace gas chromatography. Such an approach enhances both reliability and sensitivity while aligning with regulatory and sustainability objectives through reduced solvent consumption and improved method standardization. The optimized HS-GC-FID protocol for C5–C10 hydrocarbons in water complies with international performance requirements (recoveries 92–105%, RSD < 6.5%, LOQ = 0.123 μg mL^{-1}) and outperforms conventional HS-GC-FID in terms of sensitivity and reproducibility. Combined with its automation capability, minimal solvent demand, and demonstrated applicability to real samples, the method represents a robust and sustainable solution for routine environmental monitoring. While the present work was designed to optimize the overall extraction efficiency of the C5–C10 volatile fraction, future studies will be directed towards evaluating the behavior of individual hydrocarbons within this range. Applying DoE to each analyte separately may reveal compound-specific differences related to volatility or matrix interactions, thereby offering additional mechanistic insights. Such an approach could further strengthen the applicability of the method for regulatory monitoring, where both total fractions and individual components can be of environmental and toxicological relevance. The successful application of the protocol to real groundwater samples further confirms its reliability and suitability for routine environmental monitoring of volatile hydrocarbons.

Author contributions

Fabrizio Ruggieri: writing – review & editing, writing – original draft, visualization, validation, supervision, methodology, investigation, funding acquisition, formal analysis, data curation, conceptualization. Mariagiovanna Accili: validation, methodology, formal analysis, investigation, writing – original draft. Milena Casalena: validation, methodology, formal analysis, investigation, writing – original draft. Elisa Mattei: validation, methodology, formal analysis, investigation. Fabrizio Stecca: supervision, formal analysis, data curation. Mosè Lamolinara: supervision, formal analysis, methodology, data curation.

Conflicts of interest

There are no conflicts to declare.

Data availability

All data supporting the findings of this study are included within the article. No additional datasets were generated or analyzed.

Acknowledgements

The authors are grateful to the Italian Ministry for the University and Research (MUR) for funding the analytical work presented, which was carried out within the framework of the PRIN 2022 project titled "EXploitation of targeted and untargeted analytical strategies for WASTEwateR monitoring: toward a sustainable water management according to the principles of circular economy" (EXWASTER). The project is funded under Grant No. 2022L3AH34.

References

1 S. Kuppusamy, N. R. Maddela, M. Megharaj and K. Venkateswarlu, in *Total Petroleum Hydrocarbons: Environmental Fate, Toxicity, and Remediation*, Springer International Publishing, Cham, 2020, pp. 95–138.
2 P. Lambert, M. Fingas and M. Goldthorp, *J. Hazard. Mater.*, 2001, **83**, 65–81.
3 N. S. Chary and A. R. Fernandez-Alba, *TrAC – Trends Anal. Chem.*, 2012, **32**, 60–75.
4 S. Kuppusamy, K. V. Naga Raju Maddela and M. Megharaj, *Total Petroleum Hydrocarbons*, Springer Nature Switzerland, Nellore, Andhra Pradesh, India.
5 M. S. Hutcheson, D. Pedersen, N. D. Anastas, J. Fitzgerald and D. Silverman, *Regul. Toxicol. Pharmacol.*, 1996, **24**, 85–101.
6 I.-S. Park and J.-W. Park, *J. Hazard. Mater.*, 2010, **179**, 1128–1135.
7 ISO 9377, Water quality, Determination of hydrocarbon oil index Chromatography, Part 2: Method using solvent extraction and gas, 2000.
8 A. C. Soria, M. J. García-Sarrió and M. L. Sanz, *TrAC – Trends Anal. Chem.*, 2015, **71**, 85–99.
9 Z. Wang, K. Li, M. Fingas, L. Sigouin and L. Ménard, *J. Chromatogr. A*, 2002, **971**, 173–184.
10 F. S. Higashikawa, M. Luz, A. Roig, C. A. Silva and M. A. Sánchez-monedero, *Chemosphere*, 2013, **93**, 2311–2318.
11 R. Pascale, G. Bianco, S. Calace, S. Masi, I. M. Mancini, G. Mazzone and D. Caniani, *J. Chromatogr. A*, 2018, **1548**, 10–18.
12 M. J. Perkins and V. S. Langford, *Environments*, 2022, **9**(10), 124.
13 S. Kuppusamy, N. R. Maddela, M. Megharaj and K. Venkateswarlu, in *Total Petroleum Hydrocarbons: Environmental Fate, Toxicity, and Remediation*, Springer International Publishing, Cham, 2020, pp. 1–27.
14 2000/60/EC Commission Regulation (EC), *Off. J. Eur. Communities*, 2000, L. 327/1.
15 A. U. S. E. Protection, *EPA 690 Provisional Peer-Reviewed Toxicity Values for Complex Mixtures of Aliphatic and Aromatic Hydrocarbons*, Cincinnati, 2009.
16 M. K. Stenstrom, F. Sami and G. S. and Silverman, *Environ. Technol. Lett.*, 1986, **7**, 625–636.
17 C. Fang, Y. Xiong, Q. Liang, Y. Li and P. Peng, *Org. Geochem.*, 2011, **42**, 316–322.
18 R. M. Cavalcante, M. V. F. De Andrade, R. V Marins and L. D. M. Oliveira, *Microchem. J.*, 2010, **96**, 337–343.
19 N. H. Snow, S. Orange and G. C. Slack, *Trends Anal. Chem.*, 2002, **21**, 608–617.
20 M. Llompart, K. Li and M. Fingas, *J. Chromatogr. A*, 1998, **824**, 53–61.
21 A. Girme, G. Saste, S. Pawar, C. Ghule, A. Mirgal, S. Patel, A. Tiwari, S. Ghoshal, S. B. Bharate, S. S. Bharate, D. S. Reddy, R. A. Vishwakarma and L. Hingorani, *ACS Omega*, 2021, **6**, 23460–23474.
22 Z. Yang, W. Zhendi, Y. Chun, H. Bruce, B. Carl and M. and Landriault, *Environ. Forensics*, 2013, **14**, 193–203.
23 P. M. Carneiro, P. I. M. Firmino, M. C. Costa, A. C. Lopes and A. B. Dos Santos, *J. Sep. Sci.*, 2014, **37**, 265–271.
24 E. Yiantzi, K. Murtada, K. Terzidis, J. Pawliszyn and E. Psillakis, *Anal. Chim. Acta*, 2022, **1189**, 339217.
25 G. S. Douglas, W. A. Burns, A. E. Bence, D. S. Page and P. Boehm, *Environ. Sci. Technol.*, 2004, **38**, 3958–3964.
26 M. I. Cervera, J. Beltran, F. J. Lopez and F. Hernandez, *Anal. Chim. Acta*, 2011, **704**, 87–97.
27 K. Demeestere, J. Dewulf, B. De Witte and H. Van Langenhove, *J. Chromatogr. A*, 2007, **1153**, 130–144.
28 J. P. Donval, J. L. Charlou and L. Lucas, *Chemom. Intell. Lab.*, 2008, **94**, 89–94.
29 W. A. Lopes, G. O. da Rocha, P. A. P. de Pereira, F. S. Oliveira, L. S. Carvalho, N. C. de Bahia, L. S. dos Conceião and J. B. de Andrade, *J. Sep. Sci.*, 2008, 1787–1796.
30 J. Nunes, G. Nardini, J. Merib, A. Neves, E. Martendal and E. Carasek, *J. Chromatogr. A*, 2012, **1233**, 22–29.
31 S. Net, D. Dumoulin, R. El-osmani, V. Delcourt, M. Bigan and B. Ouddane, *Appl. Geochemistry*, 2014, **40**, 126–134.
32 M. Letellier, H. Budzinski, L. Charrier, S. Capes and A. M. Dorthe, *Fresenius' J. Anal. Chem.*, 1999, 228–237.
33 A. A. D'Archivio, M. A. Maggi and F. Ruggieri, *Food Anal. Methods*, 2016, **9**, 2773–2779.
34 R. Leardi, *Anal. Chim. Acta*, 2009, **652**, 161–172.
35 F. Ruggieri, A. A. D'Archivio, M. Foschi and M. A. Maggi, *Anal. Methods*, 2020, **12**, 2772–2778.